The derivation of twin laws in non-merohedric twins - Application to the analysis of hybrid twins

Massimo Nespolo, Giovanni Ferraris

electronic reprint

Acta Crystallographica Section A
Foundations of Crystallography
ISSN 0108-7673
Editor: **D. Schwarzenbach**

The derivation of twin laws in non-merohedric twins. Application to the analysis of hybrid twins

Massimo Nespolo and Giovanni Ferraris

Acta Crystallographica Section A
Foundations of Crystallography
ISSN 0108-7673

Received 1 May 2006
Accepted 21 June 2006

Dedicated to Professor H. Fuess on the occasion of his 65th birthday

The derivation of twin laws in non-merohedric twins. Application to the analysis of hybrid twins

Massimo Nespolo[a]* and Giovanni Ferraris[b]

[a]LCM3B, UMR-CNRS 7036, Université Henri Poincaré Nancy I, BP 239, F-54506 Vandœuvre-lès-Nancy CEDEX, France, and [b]Università di Torino, Dipartimento di Scienze Mineralogiche e Petrologiche, Istituto di Geoscienze e Georisorse, CNR, Via Valperga Caluso 35, I-10125 Torino, Italy. Correspondence e-mail: massimo.nespolo@lcm3b.uhp-nancy.fr

An algorithm is presented to derive the twin laws in non-merohedric twins through the systematic search for quasi-perpendicular lattice planes/directions. The twin lattice, *i.e.* the sublattice common to the whole crystalline edifice built by the twinned individuals, is based on a supercell of the individual defined by a pair of quasi-perpendicular lattice elements (*hkl*)/[*uvw*]. Starting from a (real or supposed) twin element, (*hkl*) or [*uvw*], the set of quasi-perpendicular lattice elements with user-defined limits on the twin index and obliquity is explored. The degree of lattice quasi-restoration is commonly measured by the classical twin index but in some cases, especially for large supercells, this index represents only a first approximation of the degree of lattice quasi-restoration, because more than one pair (*hkl*)/[*uvw*] may exist, and more than one concurrent sublattices of nodes, based on the same twin element, may be quasi-restored, although within different obliquities. These twins, whose existence has been recently recognized, are termed *hybrid twins*. In hybrid twins, the degree of lattice quasi-restoration is measured by the *effective twin index* n_E, a generalization of the classical twin index: in the limiting case of only one (quasi-)restored sublattice, the effective twin index and the classical twin index coincide. A number of examples previously reported simply as 'non-Friedelian' twins (with a twin index higher than the empirical limit of 6 established by Friedel) are analysed and reinterpreted as hybrid twins. A Fortran program is made available, which derives the possible twin laws according to this algorithm and analyses the pseudosymmetry of the concurrent sublattices defined by each pair (*hkl*)/[*uvw*]. The occurrence of hybrid concurrent components in twinning does not affect the normal procedures of dealing with diffraction patterns of twinned crystals.

1. Introduction

A twin is a heterogeneous edifice consisting of the oriented association of two or more homogeneous crystals (individuals); in this sense, a twin has also been defined (Ferraris *et al.*, 2004) as a modular structure at the crystal level (*cf.* a discussion in Nespolo & Ferraris, 2004*a*). The symmetry of the individuals is described by a space group $\mathcal{G}$, whereas the symmetry of the twin is identified in vector space by a point group $\mathcal{K}$ which is a supergroup of $\mathcal{H}^* = \cap_i \mathrm{H}_i$, the intersection group of the oriented vector point groups $\mathcal{H}_i$ of the individuals (Hahn & Klapper, 2003; Nespolo *et al.*, 2004). The holohedral supergroup (proper or trivial) of $\mathcal{H}$ is indicated by $\mathcal{D}(\mathcal{H})$. Let $\mathbf{L}_T$ be the twin lattice, *i.e.* the lattice common to all the individuals in the twin (Donnay, 1940). $\mathcal{D}(\mathbf{L}_T)$ is the holohedral vector point group describing the point symmetry of $\mathbf{L}_T$: depending on whether $\mathcal{K}$ is also holohedral or not, we have $\mathcal{D}(\mathbf{L}_T) \supset \mathcal{K}$ or $\mathcal{D}(\mathbf{L}_T) = \mathcal{K}$. The coset decomposition of $\mathcal{K}$ with respect to $\mathcal{H}^*$ gives the possible twin laws, each coset representing a twin law, and each operation in a coset representing a twin operation; the operations in a coset are equivalent under the operations of $\mathcal{H}^*$. Operations in $\mathcal{H}$ describe the vector point symmetry of the individuals, whereas those in the cosets obtained by decomposing $\mathcal{K}$ in terms of $\mathcal{H}^*$ connect the different individuals. To underline their different nature, the twin operations are often associated with a 'colour' and $\mathcal{K}$ is a thus a chromatic vector point group, known as the *twin point group* (Nespolo, 2004). Twins in which lattice rows common to the individuals exist in three, two or one directions are called triperiodic, diperiodic and monoperiodic, respectively (Friedel, 1933). In this study, we devote our analysis to triperiodic twins only, which are by far the largest of the three groups.

The derivation of the twin laws is a straightforward task once $\mathcal{K}$ and $\mathcal{H}$ are known or supposed. For example, in the case of twinning by syngonic merohedry, $\mathcal{K} \subseteq \mathcal{D}(\mathcal{H})$ and the

possible twin laws are obtained by coset decomposition of $\mathcal{D}(\mathcal{H})$ with respect to $\mathcal{H}^* = \mathcal{H}$. In non-merohedric twins,[1] instead, when starting from $\mathcal{H}$ the number of *possible* twin laws becomes very large: on the basis of the reticular theory of twinning (Friedel, 1904, 1926), the probability of occurrence of a twin law can be estimated by the lattice (quasi-)restoration for the individuals in the orientations $\mathcal{H}_i$, which, however, is a criterion with several exceptions. One suitable approach to derive the possible twin laws is to search for sublattices[2] of the individual lattice $\mathbf{L}_{\rm ind}$. When a sublattice has at least one symmetry element not coincident, either in type or orientation, with those of $\mathbf{L}_{\rm ind}$, it represents a possible twin lattice $\mathbf{L}_{\rm T}$, and the corresponding holohedral group is $\mathcal{D}(\mathbf{L}_{\rm T})$: again the twin laws are obtained by coset decomposition. This approach is implemented in algorithms that explore possible supercells, like *OBLIQUE* (Le Page, 2002), available in the *PLATON* package (Spek, 1990). Another approach is to search directly the possible twin elements on the basis of the lattice plane/axis (quasi-)perpendicularity, obtaining thus $\mathcal{D}(\mathbf{L}_{\rm T})$ as the final result. This is the approach we follow in the present article, and that we have implemented in the program *GEMINOGRAPHY*, described below. Geminography is the term introduced by J. D. H. Donnay to indicate the branch of crystallography dealing with twinning (Nespolo & Ferraris, 2003). To describe the algorithm implemented in the program, we need first a short theoretical excursus.

List of the symbols used in this article

$\mathbf{L}_{\rm ind}$: the lattice of the individual

$\mathbf{L}_{\rm T}$: the twin lattice; in the case of concurrent sublattices (hybrid twins), these are numbered sequentially ($\mathbf{L}_1$, $\mathbf{L}_2$ *etc.*); among these sublattices, $\mathbf{L}_{\rm T}$ is that corresponding to the lowest obliquity and is always taken as the first sublattice: $\mathbf{L}_{\rm T} = \mathbf{L}_1$

$\mathcal{H}_i$: the oriented vector point group of the ith individual

$\mathcal{H}^*$: the intersection group of the $\mathcal{H}_i$s

$\mathcal{D}(\mathcal{H})$: the holohedral supergroup (proper or trivial) of $\mathcal{H}$

$\mathcal{K}$: the vector point group relating the various individuals in the twin

$\mathcal{D}(\mathbf{L}_{\rm ind})$: the (holohedral) vector point group describing the point symmetry of $\mathbf{L}_{\rm ind}$

$\mathcal{D}(\mathbf{L}_{\rm T})$: the (holohedral) vector point group describing the point symmetry of $\mathbf{L}_{\rm T}$

$\mathbf{G}$: the metric tensor in direct space

$\mathbf{G}^*$: the metric tensor in reciprocal space

$\langle\ |$: a row matrix ('bra')

$|\ \rangle$: a column matrix ('ket')

n: the classical twin index, after Friedel (1904, 1926)

$n_{\rm max}$: the user-defined highest value of the twin index used in the exploration algorithm

ω: the twin obliquity, after Friedel (1926)

$\Lambda(n,\omega)$: region of the (n,ω) bidimensional space where concurrent sublattices built on nodes quasi-restored by the twin operation exist

$\omega_{\rm LL}$: the user-defined lower limit of the obliquity used in the exploration algorithm; default value set to 0°

$\omega_{\rm UL}$: the user-defined upper limit of the obliquity used in the exploration algorithm; default value set to 6°

$\omega_{\rm lowest}$: the lowest value of the obliquity in the interval $\omega_{\rm LL} \rightarrow \omega_{\rm UL}$ found in the exploration of the $\Lambda(n,\omega)$: $\omega_{\rm lowest} \in [\omega_{\rm LL},\omega_{\rm UL}]$

$n_{\rm E}$: the effective twin index

λ_κ: number of points in $\Lambda(\kappa,\omega)$ that correspond to sublattices

$[u^P_{A,i}v^P_{A,i}w^P_{A,i}]$, $[u^P_{B,i}v^P_{B,i}w^P_{B,i}]$: the two directions defining the primitive mesh in the ith (hkl) plane ($i = 1$ for reflection twins)

$x_Ay_Az_A$, $x_By_Bz_B$: the coordinates of the first node along the two directions defining the conventional mesh in the (hkl) plane

$[u^P_iv^P_iw^P_i]$: for reflection twins, the ith direction quasi-perpendicular to the twin plan (hkl); $[u^P_1v^P_1w^P_1]$ coincides with $[u^P_{\rm T}v^P_{\rm T}w^P_{\rm T}]$, which is the twin axis of rotation twins

$[u^C_iv^C_iw^C_i]$: the same direction as $[u^P_iv^P_iw^P_i]$ but expressed in terms of the axial setting of the conventional cell

$x_iy_iz_i$: the coordinates of the first node along the $[u^C_iv^C_iw^C_i]$ direction

$\subset$ / $\supset$: subgroup / supergroup

$\cap$ / $\cup$: intersection / union

2. Basic concepts of an extended reticular theory of crystal twinning

A *twin element* is the lattice element of $\mathbf{L}_{\rm ind}$ (plane, row, centre) about which the twin operation is performed. The twin elements are (pseudo)symmetry elements for the twin lattice $\mathbf{L}_{\rm T}$, which either coincides with $\mathbf{L}_{\rm ind}$ or is a sublattice of it. A (pseudo)symmetry plane (hkl) is (quasi-)perpendicular to a lattice row $[uvw]$, and a (pseudo)symmetry axis $[uvw]$ is (quasi-)perpendicular to a lattice plane (hkl). From the group-theoretical viewpoint, the twin operations correspond to the cosets of $\mathcal{D}(\mathbf{L}_{\rm T})$ with respect to $\mathcal{H}^*$. When $\mathbf{L}_{\rm T}$ coincides with $\mathbf{L}_{\rm ind}$, twinning is by merohedry; this is subdivided into *twinning by syngonic merohedry*, when $\mathcal{K} \subseteq \mathcal{D}(\mathcal{H})$, and *twinning by metric merohedry* when $\mathcal{K} \supset \mathcal{D}(\mathcal{H})$ (Nespolo & Ferraris, 2000.)[3] If $\mathcal{D}(\mathbf{L}_{\rm ind})$ is close to a higher holohedry $\mathcal{D}'$, the twin operation may belong to a coset of $\mathcal{D}'$ with respect to $\mathcal{D}(\mathcal{H})$: in this case, $\mathcal{D}(\mathbf{L}_{\rm T})$ is taken to coincide with $\mathcal{D}'$ and twinning is by pseudomerohedry. $\mathbf{L}_{\rm T}$ then still extends throughout the twinned edifice but has a slight deviation, corresponding to the obliquity, at the composition surface (Donnay, 1940), and because of this deviation is not, rigorously speaking, a Bravais lattice. In both cases, the restoration of $\mathbf{L}_{\rm ind}$ is complete,

[1] The expression 'non-merohedric twins' is often used to indicate all twins but those by merohedry. In this article, we use it in a slightly more restricted meaning, to indicate twins with twin index >1. To emphasize that the expression 'non-merohedral twins' often appearing in the literature is inappropriate: 'merohedral' indicates the symmetry of an individual, not that of a twin (Catti & Ferraris, 1976).

[2] A sublattice is a lattice whose translation group is a subgroup of that of the original lattice. The cell of the sublattice is thus a supercell of the original lattice. In reciprocal space, the super–sublattice relations are inverted.

[3] Friedel (1904, p. 143, 1926, pp. 56–57) stated that metric merohedry – which he called 'higher-order merohedry' (mériédrie d'ordre supérieur) – was either unlikely or equivalent to a pseudo-merohedry of low obliquity. Nowadays, several examples of true metric merohedry (within experimental uncertainty) are known.

Table 1
Classification of crystal twinning.

In the case of metric merohedry, the condition $\mathcal{K} \supset \mathcal{D}(\mathcal{H})$ implies that the twin operation belongs to $\mathcal{D}(\mathbf{L}_T)$ but not to $\mathcal{D}(\mathcal{H})$: the specialized metric has an important effect on twinning because the twin operation belongs to the higher holohedry. On the other hand, syngonic merohedry is characterized by $\mathcal{K} \subseteq \mathcal{D}(\mathcal{H})$, which implies that the twin operation belongs to $\mathcal{D}(\mathcal{H})$.

Twin index n	Obliquity ω	Relations among $\mathcal{D}(\mathbf{L}_T)$, $\mathcal{D}(\mathbf{L}_{ind})$, $\mathcal{D}(\mathcal{H})$ and $\mathcal{H}$	Extended classification	Friedel's classification
= 1	= 0	$\mathcal{D}(\mathbf{L}_T) = \mathcal{D}(\mathbf{L}_{ind}) \supseteq \mathcal{D}(\mathcal{H}) \supseteq \mathcal{K} \supset \mathcal{H}$	Syngonic merohedry	Merohedry
		$\mathcal{D}(\mathbf{L}_T) = \mathcal{D}(\mathbf{L}_{ind}) \supset \mathcal{D}(\mathcal{H})$; $\mathcal{K} \supset \mathcal{D}(\mathcal{H})$	Metric merohedry	
= 1	> 0	$\mathcal{D}(\mathbf{L}_T) \supset \mathcal{D}(\mathbf{L}_{ind})$	Pseudomerohedry	Pseudomerohedry
> 1	= 0	$\mathcal{D}(\mathbf{L}_T) \neq \mathcal{D}(\mathbf{L}_{ind})$	Reticular merohedry	Reticular merohedry
		$\mathcal{D}(\mathbf{L}_T) = \mathcal{D}(\mathbf{L}_{ind})$	Reticular polyholohedry	
> 1	> 0	$\mathcal{D}(\mathbf{L}_T) \neq \mathcal{D}(\mathbf{L}_{ind})$	Reticular pseudomerohedry	Reticular pseudomerohedry
		$\mathcal{D}(\mathbf{L}_T) = \mathcal{D}(\mathbf{L}_{ind})$†	Reticular pseudopolyholohedry	

† This relation holds when considering the idealized $\mathbf{L}_T$, as usual in TLQS.

Table 2
Condition of lattice plane/direction mutual perpendicularity in the seven lattice systems of the three-dimensional space.

See Table 1.3.2.1 in Koch (1999).

Lattice system	Lattice plane	Lattice direction
Triclinic	–	–
Monoclinic (*b*-unique)	(010)	[010]
Orthorhombic	(100)	[100]
	(010)	[010]
	(001)	[001]
Tetragonal	(001)	[001]
	(*hk*0)	[*hk*0]
Rhombohedral and hexagonal (hexagonal axes)	(0001)	[001]
	(*hki*0)	[2*h*+*k*,*h*+2*k*,0]
Cubic	(*hkl*)	[*hkl*]

although in the second case it is only approximate: one says that the *twin index* is 1.

When $\mathbf{L}_T$ is a sublattice of $\mathbf{L}_{ind}$ the degree of (quasi-) restoration of $\mathbf{L}_{ind}$ is lower: twinning is by reticular merohedry, the twin index n is higher than 1 and corresponds to the ratio of the volumes of the primitive cells of the two lattices. If $\mathcal{D}(\mathbf{L}_T)$ is close to a higher holohedry $\mathcal{D}'$, the twin operation may belong to a coset of $\mathcal{D}'$ with respect to $\mathcal{D}(\mathcal{H}^*)$: in this case, $\mathcal{D}(\mathbf{L}_T)$ is taken to coincide with $\mathcal{D}'$ and twinning is by reticular pseudomerohedry. Exactly as in the case of twinning by pseudomerohedry, $\mathbf{L}_T$ is not, rigorously speaking, a Bravais lattice.

Without losing generality, the analysis of the relation between $\mathbf{L}_T$ and $\mathbf{L}_{ind}$ to obtain the possible twin laws in non-merohedric twins can be limited to the case where both the twin and the individual are holohedral, and $\mathcal{H}^*$ is centrosymmetric. In other words, in the following we assume $\mathcal{K} = \mathcal{D}(\mathbf{L}_T)$, $\mathcal{H} = \mathcal{D}(\mathcal{H})$ and $\mathcal{H}^* = \cap_i \mathcal{D}(\mathbf{L}_{ind})_i$. The derivation of the twin laws is thus a matter of decomposing $\mathcal{D}(\mathbf{L}_T)$ in terms of $\mathcal{H}^*$: each coset obtained in this way contains an equal number of operations of the first and of the second sort and the lattice (quasi-)restoration can thus be described by rotation or by reflection. This is equivalent to saying that, because a twin element is a (pseudo)symmetry element of $\mathbf{L}_T$ and because a lattice is by definition centrosymmetric, there always exists a rational element (quasi-)perpendicular to the twin element. The cell of $\mathbf{L}_T$ is finally defined by the pair (*hkl*)/[*uvw*] composed of the twin element and the reticular element quasi-perpendicular to it; the indices are expressed in the crystallographic basis of $\mathbf{L}_{ind}$. The twin index is calculated as

$$\begin{aligned} n &= X/f \\ X &= |uh + vk + wl|, \end{aligned} \tag{1}$$

where $f = 1$, 2 or 4 depending on the Bravais-lattice type and the parities of X, u, v, w, h, k, l (see, for example, Nespolo & Ferraris, 2005).[4] When u, v, w, h, k, l are expressed in terms of a primitive basis of $\mathbf{L}_{ind}$, $f = 1$ or 2 depending on whether X is even or odd. The complete classification of twinning is given in Table 1: for details of the classification, see Nespolo & Ferraris (2004*a*) and Grimmer & Nespolo (2006). A coarser classification was introduced by Donnay & Donnay (1974), who distinguished between zero-obliquity twins (twin lattice symmetry: TLS) and non-zero obliquity twins (twin lattice quasi-symmetry: TLQS). The conditions of plane/direction perpendicularity for each lattice system[5] were given by Donnay & Donnay (1959). In the cubic lattice system, each lattice row [*uvw*] is perpendicular to the lattice plane with the same indices ($h = u$, $k = v$, $l = w$); this implies a potentially very high number of TLS twin laws but their actual occurrence is limited by the fact that most of them would correspond to a high twin index. For each twin plane (axis), the perpendicular lattice element, defining the cell of $\mathbf{L}_T$, is thus immediately obtained, and the obliquity is zero. In the other lattice systems, only some pairs of lattice plane/direction are mutually perpendicular because of the lattice symmetry, independently from any metric parameter or the experimental conditions (T,p), as far as these do not imply a transition to a different lattice system. The mutually perpendicular pairs in each lattice system of the three-dimensional space are summarized in Table 2 (see Donnay & Donnay, 1959). When the cell of $\mathbf{L}_T$ is defined by a pair of lattice elements of this type, the obliquity is necessarily zero: we propose to call this type of twinning

[4] The variable X in equation (1) is more commonly indicated as S. To avoid any possible confusion with the lattice type S, we prefer to adopt here a different letter.
[5] For an explanation of the difference between lattice system and crystal system, see Wondratschek (2002). In previous editions of *International Tables for Crystallography*, lattice systems were called 'Bravais systems'.

intrinsic TLS, shortened to *i*-TLS. In all other cases, the conditions of perpendicularity, and thus the obliquity, depend on one or more metric parameters (see, for example, Grimmer, 2003; Grimmer & Kunze, 2004). In other words, a pair of elements $(hkl)/[uvw]$ may correspond to TLS or to TLQS depending on the experimental conditions determining the metric of $\mathbf{L}_{\rm ind}$. We propose to call *extrinsic* TLS, shortened to *e*-TLS, twinning in which the zero obliquity is not a consequence of the symmetry of $\mathbf{L}_{\rm ind}$ but comes instead from the particular metric of $\mathbf{L}_{\rm ind}$. Evidently, the obliquity is exactly zero in the case of *i*-TLS, whereas it is zero within the experimental error in the case of *e*-TLS.

The direction $[u'v'w']$ perpendicular to a lattice plane (hkl) and the plane $(h'k'l')$ perpendicular to a lattice row $[uvw]$ are obtained from the metric tensors $\mathbf{G}$ (in direct space) and $\mathbf{G}^*$ (in reciprocal space) (Grimmer & Nespolo, 2006; see also Friedel, 1926; Donnay & Donnay, 1959):

$$|u'v'w'\rangle = \mathbf{G}^*|hkl\rangle \tag{2}$$

$$|h'k'l'\rangle = \mathbf{G}|uvw\rangle. \tag{2'}$$

If (hkl) is a (supposed) twin plane, one speaks of reflection twin and $[u'v'w']$ is the direction perpendicular to it; if $[uvw]$ is a (supposed) twin axis, one speaks of rotation twin and $(h'k'l')$ is the plane perpendicular to it. In general, $[u'v'w']$ and $(h'k'l')$ are not rational;[6] the angle between $[u'v'w']$ and the lattice row $[uvw]$, or between $(h'k'l')$ and the lattice plane (hkl), chosen to form the $(hkl)/[uvw]$ pair is the obliquity ω, which is computed in terms of $[uvw]$ and $[hkl]^*$:

$$\cos\omega = \frac{uh + vk + wl}{L(uvw)L^*(hkl)} \tag{3}$$

where $L(uvw) = \langle uvw|\mathbf{G}|uvw\rangle^{1/2}$ and $L^*(hkl) = \langle hkl|\mathbf{G}^*|hkl\rangle^{1/2}$ are the periods of the corresponding directions (see Grimmer & Nespolo, 2006).

2.1. Structure *versus* lattice in the general analysis of twins

The actual occurrence of a twin depends on both thermodynamic and kinetic conditions (Buerger, 1945; Nespolo & Ferraris, 2004*b*), the key factor being the structural match at and near the composition surface. In some cases, the structure match is realized only for part of the structure, especially large atoms (Takeda *et al.*, 1967): the twin is then well rationalized in terms of a *restoration index*, defined similarly to the twin index but concerning a subset of atoms instead of the lattice nodes. The analysis of the structure at the boundary makes use of the diperiodic groups (Holser, 1958) and requires the knowledge of the structure in the orientations corresponding to the twin individuals. Whatever approach one chooses to analyse the structural aspects of twins, the study almost reduces to a case-by-case analysis.

On the other hand, the reticular analysis of twins allows us to abstract from the specificity of each structure by means of a general concept, the *twin lattice*. Whereas this analysis cannot explain all the observations on the occurrence frequency of twins, it supplies nevertheless a general criterion to explain and foresee most twins. In fact, a high degree of (quasi-) restoration of lattice nodes is favourable to the formation of twins (see *e.g.* Santoro, 1974) because it implies a good continuity of the structural motif in the different non-equivalent orientations of the individuals brought to (quasi-) coincidence by the twin operations.

2.2. Non uniqueness of $\mathbf{L}_{\rm T}$ in TLQS

The experimentally observed (or theoretically expected) twin law gives the twin plane (axis), which in turn defines the cell of $\mathbf{L}_{\rm T}$ once the (quasi-)perpendicular lattice row (plane) has been determined. In TLQS, the cell of $\mathbf{L}_{\rm T}$ can in principle be chosen in different ways because, for a given twin plane (axis), different quasi-perpendicular pairs $(hkl)/[uvw]$ can be found, the direction (plane) exactly perpendicular being irrational. In other terms, unless the value of the obliquity is known *a priori* from some experimental or theoretical considerations, the choice of $\mathbf{L}_{\rm T}$ is not straightforward. For example, the *Breithaupt* twin $\{11\bar{2}1\}$ in β-quartz was described in two different ways by Friedel (1923), who used the pair $(11\bar{2}1)/[552]$ in the table on page 92 because of the lower obliquity but eventually opted for the pair $(11\bar{2}1)/[221]$ in the text because of the lower twin index.

If the obliquity is known, for example estimated from the separation of split diffractions, it can be used as a minimal value of ω to be accepted during the exploration of the $(hkl)/[uvw]$ pairs: for this reason, the algorithm described below requires in input an $\omega_{\rm LL}$ (lower limit) value. The exploration of the direct space for pairs of quasi-perpendicular $(hkl)/[uvw]$ is done between $\omega_{\rm LL}$ and $\omega_{\rm UL}$ (upper limit); when the obliquity is unknown, $\omega_{\rm LL}$ is set to zero and instead an internal criterion has to be applied for the choice of $\mathbf{L}_{\rm T}$. Different lattice rows (planes) quasi-perpendicular to the twin element may correspond to largely different twin indices and this difference simply rules out all but one candidate. When such a clear-cut situation does not exist, the quasi-perpendicular pair defining $\mathbf{L}_{\rm T}$ is not evident and different choices are then possible: the choice of a threshold is described in §4.1.

2.3. Hybrid twinning

From the lattice viewpoint, a twin operation brings to (quasi-)superposition rational directions that are not equivalent – all or part – under $\mathcal{H}$: along these directions, the structure must fit sufficiently well in order to obtain a crystalline edifice. The degree of lattice (quasi-)restoration is inversely related to the twin index and the obliquity; a large part of known non-merohedric twins correspond to low obliquity and low twin index, the empiric limiting values being 6° for the obliquity and 6 for the twin index (Friedel, 1926). Twins that correspond to this criterion are called 'Friedelian twins' (Nespolo & Ferraris, 2005).

A number of examples of non-Friedelian twins are known, which are hardly understandable on the basis of the classical reticular theory. Actually, many of them can again be

[6] These are obviously rational elements in the reciprocal space. Nevertheless, Mallard's law (Friedel, 1926) states that a twin element must be a lattice element in direct space.

rationalized in terms of the lattice (quasi-)restoration, provided the classical approach is extended to consider the coexistence of N quasi-restored sublattices $\mathbf{L}_i$, $i = 1, \ldots, N$. These concurrent sublattices correspond to the same twin law, are defined by different pairs $(hkl)/[uvw]$, all based on the common twin element and differing for the quasi-perpendicular lattice element, and show different degrees of quasi-restoration. Among the N concurrent sublattices, the one corresponding to the lowest obliquity defines $\mathbf{L}_T$ and is hereafter taken as first sublattice in the numbering of sublattices: $\mathbf{L}_1 = \mathbf{L}_T$. In TLS, the lowest obliquity is zero, whereas in TLQS it is not defined *a priori* because, as discussed in the previous section, the choice of $\mathbf{L}_T$ may not be straightforward. When the user gives a non-zero value of ω_{LL}, the search for concurrent sublattices is limited to $\omega_{lowest} \geq \omega_{LL}$; when there is no experimental estimation of ω_{LL}, alternative criteria to end the exploration of sublattices are used instead, and are described in §4.1. The concurrent sublattices can be found by searching for all the elements of $\mathbf{L}_{ind}$ that are quasi-perpendicular to the twin element, where 'quasi' means within the accepted obliquity. The nature of the twin element is not affected: it is only the *description* of the lattice quasi-restoration that changes when considering concurrent sublattices.

The indices $u'v'w'$ (or $h'k'l'$) of the direction (or plane) perpendicular to the twin element can always be brought – with some numerical tolerance – to coprime integers uvw (or hkl) but the values obtained in this way may be so high that they simply do not correspond to a rational element. Even when they do, however, the corresponding twin index may be too high and represent thus a negligible degree of lattice (quasi-)restoration. The latter should take into account all nodes that are quasi-restored in the range of the accepted obliquity ($\omega_{LL} \rightarrow \omega_{UL}$), not only those that are restored within the lowest obliquity ($\omega = 0$ in TLS). When more than one quasi-restored concurrent sublattices $\mathbf{L}_i$ exist in the $\omega_{LL} \rightarrow \omega_{UL}$ range, the classical twin index represents only a *first approximation* of the overall degree of lattice quasi-restoration. In fact, the lattice element (direction/plane) corresponding to the lowest obliquity may define a rather large cell for $\mathbf{L}_T$. In a case like this, to describe the degree of lattice quasi-restoration by means of only one sublattice actually means to underestimate it.

To address this category of twins, we have recently introduced the definition of *hybrid twins* as twins in which more than one quasi-restored concurrent sublattices exist for $\omega < \omega_{UL}$ (Nespolo & Ferraris, 2005). In our previous study, the overall degree of lattice quasi-restoration was described by up to three concurrent sublattices:

1. $\mathbf{L}_T$, corresponding to the lowest obliquity;

2. the first alternative sublattice ($\mathbf{L}_A$), based on the twin element under consideration and an alternative quasi-perpendicular element;

3. the second alternative sublattice ($\mathbf{L}_B$), based on the (quasi-)perpendicular element of $\mathbf{L}_T$ and an alternative twin element.

To measure the degree of lattice quasi-restoration, we introduced the concept of *effective twin index* n_E, which is a function of the twin indices of the three concurrent sublattices. The effective twin index as defined by Nespolo & Ferraris (2005) represents a *better approximation* of the degree of quasi-restoration than the classical twin index but it does not correspond yet to the full set of quasi-restored nodes. In fact, it takes into account only the sublattice corresponding to the lowest obliquity and that corresponding to the lowest twin index for $\omega < \omega_{UL}$. The introduction of the $\mathbf{L}_B$ sublattice was aimed at improving the degree of approximation, but in some cases it may turn out to give misleading results: for example, the $\mathbf{L}_B$ sublattice of the Belowda Beacon twin in β-quartz would correspond to the pair $(10\bar{1}1)/[211]$, which on the other hand defines the $\mathbf{L}_T$ sublattice of the Esterel twin. For all these reasons, we proceed to refine the definition of the effective twin index before presenting the computation algorithm.

3. Choice of concurrent sublattices and definition of the effective twin index

The following analysis is applied starting from the standard primitive cell of the individual [the one obtained from the conventional cell by the transformations in Arnold (2002)].

The two parameters n and ω (twin index and obliquity) define a two-dimensional region, whose boundaries are fixed by the largest acceptable twin index n_{max} and by the lower and upper limits on the obliquity, ω_{LL} and ω_{UL}. It is in this region $\Lambda(n_{max},\omega_{LL}\rightarrow\omega_{UL})$ that sublattices have to be found. Let λ be the integer number of points in the $\Lambda(n,\omega)$ region that correspond to sublattices. For a given twin element, $\lambda \geq 0$; when $\lambda = 0$, the lattice element under investigation is not a possible twin element for a triperiodic twin, at least within the fixed boundaries. The direction in $\Lambda(n,\omega)$ corresponding to the lowest ω defines the cell of $\mathbf{L}_T$; other directions – if any – corresponding to the same n but to a higher ω are not taken into account because the first node along such a direction is external to the cell of $\mathbf{L}_T$. The degree of (quasi-)restoration of the lattices of the individuals is measured by the fraction of nodes of this cell that are approximately restored by the twin operation, where 'approximately' means within ω_{UL}. The totality of quasi-restored nodes are those belonging to the cells represented by points in the $\Lambda(n_{max},\omega_{LL}\rightarrow\omega_{UL})$ region.

Because the choice of n_{max} and ω_{UL} is *a priori* without constraints, the degree of lattice quasi-restoration and the value of λ in principle are not uniquely defined: by enlarging the $\Lambda(n,\omega)$ region a different result may be found. This is typically what happens when analysing a high-index twin: one passes from $\lambda = 0$ in the Friedelian region $\Lambda(6,6^\circ)$ to $\lambda > 0$ in a larger region $\Lambda(n>6,6^\circ)$. Even in the Friedelian region $\Lambda(6,6^\circ)$ some twins actually show $\lambda > 1$: this means that the sublattice normally chosen to describe $\mathbf{L}_T$ corresponds to the lowest value of either n or ω, but not of both; there is then at least another sublattice whose contribution to the lattice quasi-restoration is not negligible. In cases like this, the description as hybrid twin gives a better account of the overall degree of lattice quasi-restoration.

The number of points λ in $\Lambda(n,\omega)$ depends on the choice of ω_{UL}; this parameter is however limited to physically

meaningful values. In fact, a non-zero value of the obliquity means that the farther we move from the composition surface separating the individuals the more approximate is the lattice quasi-restoration. If the obliquity is high, the lattice mismatch becomes more severe also in proximity to the composition surface. Once the λ concurrent sublattices in $\Lambda(n,\omega)$ have been located, the overall degree of lattice quasi-restoration is measured by the ratio between the multiplicity of the cell of $\mathbf{L}_T$ and the number of lattice nodes in this cell that belong to the $\mathbf{L}_i$ concurrent sublattices. These (quasi-)restored nodes define the effective twin index n_E. An *estimation* of n_E is given by the following expression:

$$\langle n_E \rangle = \frac{X_1}{\sum_{i=1}^{\lambda} \mathrm{int}(X_1/X_i) f_i}, \qquad (4)$$

where X_i and f_i are the values of X and f in equation (1) for the ith sublattice and int(x) is the integer part of x. Actually, equation (4) gives the fraction of nodes of $\mathbf{L}_{ind}$ in the cell of $\mathbf{L}_T$ belonging to the λ concurrent sublattices found in $\Lambda(n,\omega)$ and represents the lower limit of n_E. In some cases, a quasi-restored node may belong to two different sublattices, and the effective twin index may thus be slightly larger than the estimation obtained by equation (4): we will discuss this point when analysing some examples (see §§4.3.2 and 5.8).

Equation (4) is a generalization of the original definition introduced by Nespolo & Ferraris (2005): in the previous definition, the calculation of the effective twin index was straightforward and the algorithm did not include any risk of counting a node more than once. In the present extension, which aims at obtaining a more precise estimation of the actual degree of quasi-restoration of lattice nodes in hybrid twins, such a possibility exists, although only in special cases, and has to be taken into account in the calculation of n_E.

For a lattice element supposed to give rise to a non-merohedric twin, the following three cases may arise:

- $\lambda = 0$: the lattice element under investigation is not a possible twin element for a triperiodic twin, at least within n_{max}, ω_{UL};
- $\lambda = 1$, $n_E = n$: there is only one sublattice within n_{max}, ω_{UL} and the twin is *non-hybrid*; if n and ω are within the classical limits (6,6°) the pair (*hkl*)/[*uvw*] represents a *Friedelian twin*; if n and ω are not within the classical limits (6,6°) the pair (*hkl*)/[*uvw*] represents a *non-Friedelian twin* which cannot be explained as hybrid;
- $\lambda > 1$: the twin is *hybrid*, and its description as classical twin ($\lambda = 1$) is only an approximation; the degree of approximation can be estimated by the difference between n and n_E.

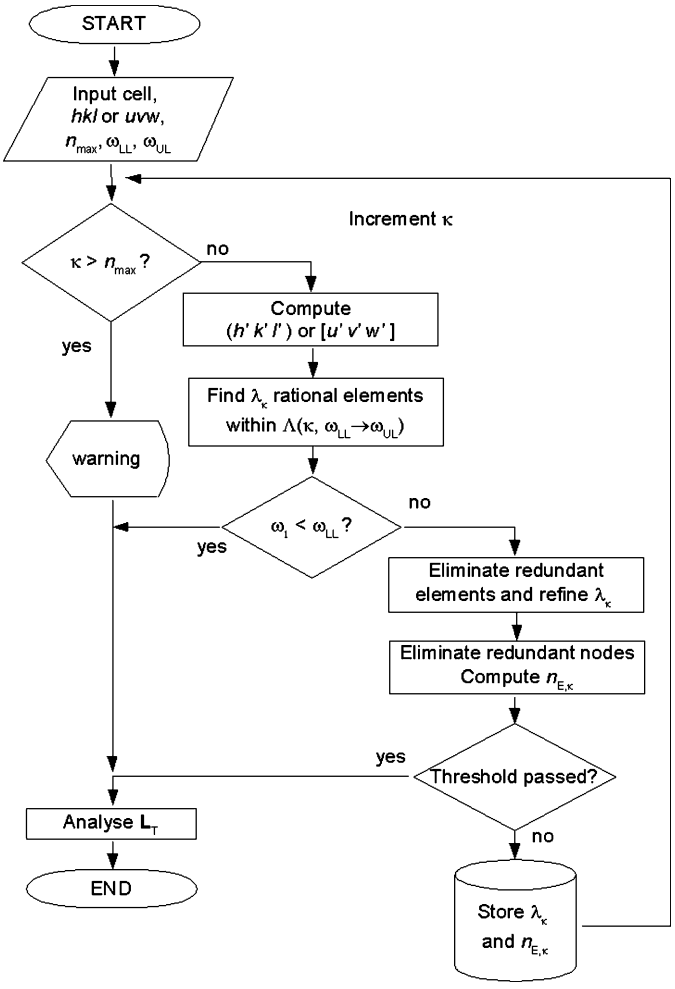

Figure 1
Schematic flowchart of the computation algorithm. For *i*-TLS twins, the computation is performed in one step, by taking $\kappa = n_{max} = X/f$ and $\omega_{LL} = 0$.

4. Exploring the $\Lambda(n,\omega)$ region

The algorithm used in the program *GEMINOGRAPHY* to explore the $\Lambda(n,\omega)$ region is described in this section. A schematic flowchart of the computation process is shown in Fig. 1.

For a given metric, defined by the lattice parameters, a user-defined twin element (*hkl*) or [*uvw*] is analysed within the user-chosen region $\Lambda(n_{max},\omega_{LL}\rightarrow\omega_{UL})$. It is also possible to explore intervals of *hkl* or *uvw*: this is useful to search for possible twin elements in a given $\mathbf{L}_{ind}$. The value of n_{max} must be definitely higher than the classic Friedelian value, otherwise most hybrid twins will not be found and the result will be simply $\lambda = 0$ or 1. For TLS twins, the cell of $\mathbf{L}_T$ is uniquely defined by the pairs (*hkl*)/[*uvw*] corresponding to zero obliquity. In the case of *i*-TLS, the value of n_{max} itself is imposed by the perpendicularity of these elements: it is automatically set at X/f, which overcomes the user-defined value, ω_{LL} is also set to zero. For *e*-TLS, the cell of $\mathbf{L}_T$ is defined by the pairs corresponding to $\omega = 0$; but, because the perpendicularity of these elements depends on at least one metric parameter, a tolerance on the zero obliquity is introduced. For TLQS, the user-defined minimal value of the obliquity, ω_{LL}, is used as a threshold to end the exploration when a direction making an obliquity lower than the one experimentally determined is reached. When an experimental estimation of the obliquity is not available, the default value of zero is used for ω_{LL} and a different threshold criterion, described below, is then used.

The $\Lambda(n,\omega)$ region is explored at once for *i*-TLS, and step-by-step for *e*-TLS and TLQS, the step pointer being hereafter indicated by κ. The perpendicular elements $(h'k'l')$ or $[u'v'w']$ are computed by means of equation (2) or (2′): these are in general irrational planes/directions. The rational elements close to $(h'k'l')$ or $[u'v'w']$ are then obtained, within the region $\Lambda(\kappa,\omega_{LL}\rightarrow\omega_{UL})$: their number is λ_κ. Not all these elements are however independent: redundant elements must be eliminated to obtain the final value of λ_κ, which is then stored, together with the effective twin index at the κth step, $n_{E,\kappa}$.

As discussed above, in TLQS twins the cell of $\mathbf{L}_T$ may not be uniquely defined: the pair defining the cell of $\mathbf{L}_T$ within a given $\Lambda(n,\omega)$ region becomes one of the alternative pairs within a larger $\Lambda(n,\omega)$ region. The consequence is that the degree of lattice quasi-restoration increases monotonously and, consequently, the effective twin index decreases. This increase in λ_κ is however not always meaningful: for a given obliquity, the linear separation between quasi-restored nodes increases with the distance from the composition surface.

To overcome this problem, two options are left to the user.

1. To choose a non-zero value of the minimal obliquity ω_{LL} below which the pairs $(hkl)/[uvw]$ are not accepted as possible cells for $\mathbf{L}_T$. This is the case when the obliquity is known or supposed. The algorithm is then used to look for possible hybrid contributions. If the twin element under consideration corresponds to *i*-TLS, ω_{LL} is forced to zero.

2. To allow the program optimizing the description of the lattice overlap by means of the algorithm described in the next section, which concerns TLQS twins analysed with $\omega_{LL} = 0$.

4.1. Choice of $\mathbf{L}_T$ for $\omega_{LL} = 0$ in TLQS

In general, λ_κ does not increase continuously at each increment of κ but may remain constant in more or less large subregions. In other words, the change between two given values of λ may occur in several steps, each step involving a small increment in the Λ region, or in one step, corresponding to a large increment of Λ. In the first case, each widening of the Λ region corresponds to a better approximation by n_E of the real degree of lattice overlap. In the second case, the additional points found in the larger Λ region correspond to contributions from nodes away from the composition surface and their physical meaning is thus negligible. In the case of reflection twins, let the period along the direction $[uvw]$ defining the *primitive* cell of $\mathbf{L}_T$ at the step κ be $\tau_{[uvw],\kappa}$: if $[uvw]$ defines a centred cell, the corresponding primitive direction is used to compute $\tau_{[uvw]}$. The ratio $\tau_{[uvw],\kappa}/\tau_{[uvw],\kappa-1}$ is taken as a threshold to stop the exploration: once outside the Friedelian region ($n > 6$), when this ratio is higher than a given threshold, the increase in the number λ of concurrent sublattices concerns lattice vectors sufficiently far from the composition surface for their contribution to be negligible. An empirical value of 1.5 for the threshold has shown to work well for all the cases analysed so far. If this limit is not reached during the whole exploration, the $\Lambda(n,\omega)$ region indicated by the user may be too narrow: a warning is then printed.

For rotation twins, $d_{(hkl)\kappa-1}/d_{(hkl),\kappa}$ is used as threshold. The smaller is $d_{(hkl)}$, the lower is the density of nodes in the plane defining the jth sublattice $\mathbf{L}_j$. Outside the Friedelian region ($n > 6$), when the above ratio is higher than 1.5, the increase in the number λ of concurrent sublattices concerns lattice planes of sufficiently low density for their contribution to be negligible.

4.2. Derivation of the quasi-perpendicular lattice elements

For each (hkl), the perpendicular direction $[u'v'w']$ is computed by means of equation (2); in the case of rotation twins, $(h'k'l')$ is computed in terms of $[uvw]$ by means of equation (2′). The algorithm works similarly on both rotation and reflection twins and one does not need to distinguish them at this stage; let us indicate the result as e_1, e_2, e_3. The algorithm proceeds as follows. An index e_j is considered to be a 'quasi-integer' if its mantissa is lower than 0.1 or higher than 0.9.

1. When e_1, e_2, e_3, are not quasi-integers – that is the general case – they are first of all normalized to the smallest of the three (e_{min}): the smallest e_j is now 1. If the two others are quasi-integers, the process jumps to step 3.

2. Let m_j be the mantissa of e_j; the three e_js are normalized to the largest m_j and the process is repeated until all the three e_js are quasi-integer, or until n_κ – the twin index computed at the κth iteration step by taking the integers closest to e_js – is larger than the limit given in input by the user (n_{max}).

3. The rational elements whose indices are closest to $e_1e_2e_3$ are computed by adding 0 ± 0.5 to each e_j in all possible combinations. The ± 0.5 addition justifies considering as 'quasi-integer' an e_j differing from an integral value by no more than 0.1. For each element obtained in this way, n and ω are computed. If they correspond to a point in the $\Lambda(n,\omega)$ region, then the corresponding element is stored.

4. The e_js are divided by $(1 + m_{max})$, where m_{max} is the largest of the three mantissas. Iteration between steps 3 and 4 continues until the smallest e_j is lower than 1. In this way, the whole set of rational elements close to the one found at step 2 is analysed.

5. The pairs $(hkl)/[uvw]$ obtained above are analysed. If no pair has been stored, then the element under consideration is not a possible twin element in the $\Lambda(n,\omega)$ region under investigation ($\lambda = 0$). Otherwise, the pair corresponding to the lowest obliquity and to the lowest n with the same ω is retained and defines the $\mathbf{L}_T$ sublattice at step κ.

4.3. Redundancy elimination and calculation of the effective twin index

At each step κ, the set of λ_κ quasi-perpendicular lattice elements is checked for consistency to avoid counting more than once a sublattice or a lattice node.

4.3.1. Elimination of the redundant pairs. In some cases, it may happen that the exploration of the $\Lambda(n_{max},\omega_{LL}\rightarrow\omega_{UL})$ region leads to counting the same sublattice more than once. This is for example the case of reflection twins when the *i*th

pair $(hkl)/[u_iv_iw_i]$ defines a centred cell and the centring vector is parallel to the $[u_jv_jw_j]$ vector defining the cell of the jth pair $(hkl)/[u_jv_jw_j]$ ($i \neq j$). For this reason, the set of quasi-perpendicular pairs obtained from the exploration of $\Lambda(n_{\max},\omega_{\rm LL}\rightarrow\omega_{\rm UL})$ is analysed to eliminate multiple sublattice counts.

For reflection twins, $\mathbf{L}_i$ is based on the twin plane (hkl) and on the ith quasi-perpendicular direction $[u_iv_iw_i]$. The elimination of redundant pairs is performed by comparing the corresponding primitive cells, which are obtained as follows.

1. A provisional cell is built, based on the primitive mesh in (hkl) corresponding to the two shortest in-plane vectors corresponding to the directions $[u_Av_Aw_A]$ and $[u_Bv_Bw_B]$ and the quasi-perpendicular direction $[u_iv_iw_i]$. Because the mesh in (hkl) is primitive, the value of $f = X/n$ for this cell can be only 1 or 2. If $f = 1$, the cell is primitive and computation jumps to step 3.

2. If $f = X/n = 2$, the cell is of type S or I; the corresponding primitive cell is obtained by computing the indices of the three directions $[u_i + u_A, v_i + v_A, w_i + w_A]$, $[u_i + u_B, v_i + v_B, w_i + w_B]$ (for S centring) and $[u_i + u_A + u_B, v_i + v_A + v_B, w_i + w_A + w_B]$ (for I centring). Only one of these three triples has all-even values: it identifies the centring vector, whose coordinates uvw are half the all-even indices found in this way.

3. The node corresponding to the vector defining the primitive cell of $\mathbf{L}_i$, whose coordinates uvw have been obtained in the previous steps, is stored together with its eight neighbours obtained by adding and subtracting the vectors defining the primitive mesh in (hkl) as well as their vector sum: $u \pm u_A, v \pm v_A, w \pm w_A$, $u \pm u_B, v \pm v_B, w \pm w_B$ and $u \pm u_A \pm u_B, v \pm v_A \pm v_B, w \pm w_A \pm w_B$.

4. The nodes obtained in this way are compared one-to-one: if the same node occurs in correspondence of more than one $\mathbf{L}_i$, only the sublattice with lower index is retained.

For rotation twins, the same analysis is applied in the reciprocal space by exchanging the role of planes and directions. Because of the relations of reciprocity of lattice types, if the reciprocal of a cell contains nodes belonging to another cell, the same is true also for the original cell.

4.3.2. Elimination of the redundant nodes and calculation of $n_{\rm E}$

Once the set of the λ independent pairs has been established, the number of nodes of $\mathbf{L}_{\rm ind}$ that are quasi-restored by the twin operation and that are internal to the cell of $\mathbf{L}_{\rm T}$ is calculated. To do this, three lattice directions are used for each sublattice $\mathbf{L}_i$:

- for reflection twins, the two directions defining a primitive mesh in the twin plane, $[u_A^Pv_A^Pw_A^P]$ and $[u_B^Pv_B^Pw_B^P]$, and the ith quasi-perpendicular direction $[u_i^Pv_i^Pw_i^P]$;
- for rotation twins, the twin axis $[u_1^Pv_1^Pw_1^P]$ and two directions defining a primitive mesh in the ith quasi-perpendicular plane $[u_{A,i}^Pv_{A,i}^Pw_{A,i}^P]$ and $[u_{B,i}^Pv_{B,i}^Pw_{B,i}^P]$.

For each triple of directions, the corresponding nodes and their neighbours are searched and stored:

- for reflection twins, stored nodes are: $u_i^Pv_i^Pw_i^P$; $u_i^P \pm u_A^P, v_i^P \pm v_A^P, w_i^P \pm w_A^P$; $u_i^P \pm u_B^P, v_i^P \pm v_B^P, w_i^P \pm w_B^P$; $u_i^P \pm u_A^P \pm u_B^P, v_i^P \pm v_A^P \pm v_B^P, w_i^P \pm w_A^P \pm w_B^P$;
- for rotation twins, stored nodes are: $u_{A,i}^P, v_{A,i}^P, w_{A,i}^P$; $u_{B,i}^P, v_{B,i}^P, w_{B,i}^P$; $u_{A,i} \pm u_1^P, v_{A,i} \pm v_1^P, w_{A,i} \pm w_1^P$; $u_{B,i}^P \pm u_1^P, v_{B,i}^P \pm v_1^P, w_{B,i}^P \pm w_1^P$; $u_{A,i}^P \pm u_{B,i}^P, v_{A,i}^P \pm v_{B,i}^P, w_{A,i}^P \pm w_{B,i}^P$; $u_{A,i}^P \pm u_{B,i}^P \pm u_1^P, v_{A,i}^P \pm v_{B,i}^P \pm v_1^P, w_{A,i}^P \pm w_{B,i}^P \pm w_1^P$.

If the cell of $\mathbf{L}_i$ is of type S or I, a further set of nodes, obtained from the centring node $u_Cv_Cw_C$, is added too.

The cell of $\mathbf{L}_{\rm T}$ contains $m = {\rm int}(X_1/X_i)$ cells of the ith sublattice. Therefore, the following nodes are added to the set obtained above:

- for reflection twins, the nodes $j \times u_i^P, j \times v_i^P, j \times w_i^P$ and $j \times u_{C,i}, j \times v_{C,i}, j \times w_{C,i}$, as well as their neighbours, j taking values from 2 to m;
- for rotation twins, the nodes $j \times u_{A,i}^P$, $j \times v_{A,i}^P$, $j \times w_{A,i}^P$; $j \times u_{B,i}^P$, $j \times v_{B,i}^P$, $j \times w_{B,i}^P$; $j \times u_{C,i}$, $j \times v_{C,i}$, $j \times w_{C,i}$, as well as their neighbours, j taking values from 2 to m.

The set of nodes obtained in this way is re-indexed in the cell of $\mathbf{L}_{\rm T}$ by applying the transformation

$$\begin{bmatrix} u_{A,1}^P & u_1^P & u_{B,1}^P \\ v_{A,1}^P & v_1^P & v_{B,1}^P \\ w_{A,1}^P & w_1^P & w_{B,1}^P \end{bmatrix}^{-1} \left| u \quad v \quad w \right\rangle_{\mathbf{L}_{\rm ind}} = \left| u \quad v \quad w \right\rangle_{\mathbf{L}_{\rm T}}. \quad (5)$$

Only the nodes $|uvw\rangle_{\mathbf{L}_{\rm T}}$ having all the three coordinates non-negative and less than 1 are in the cell of $\mathbf{L}_{\rm T}$. Among these, if a node occurs twice or more, it is counted only once. The effective twin index $n_{\rm E}$ is finally obtained by dividing the multiplicity of the cell of $\mathbf{L}_{\rm T}$ by the number of nodes obtained in this way.

4.4. Analysis of the pseudosymmetry of the twin lattice

The analysis of the symmetry of a lattice is a straightforward task best accomplished *via* the metric tensor (see *e.g.* Mighell & Rodgers, 1980). In the case of twins, however, we are more interested in the *pseudo*symmetry of $\mathbf{L}_{\rm T}$ rather than in its true symmetry. In fact, to say that a (sub)lattice $\mathbf{L}_i$ is restored within a given obliquity ω implicitly means that the symmetry of that sublattice, $\mathcal{D}(\mathbf{L}_i)$, is close to a higher holohedry $\mathcal{D}'$, the discrepancy being at most ω. The proximity of the linear parameters is also important in evaluating the pseudosymmetry of a (sub)lattice. For example, an orthorhombic crystal with a numerically close to b may undergo twinning by $\pm 90^\circ$ rotation about the c axis. The twin law is the coset obtained when decomposing $\mathcal{D}(\mathbf{L}_{\rm T}) = 4/mmm$ in terms of $\mathcal{D}(\mathcal{H}) = mmm$, and – from the view point of the lattice – any of the eight operations in this coset (including the operation $4_{[001]}$ for which the obliquity is zero)[7] may be taken as twin operation. In a case like this, $\mathbf{L}_{\rm T}$ coincides with $\mathbf{L}_{\rm ind}$ within $|a - b|$.

The (pseudo)symmetry of $\mathbf{L}_{\rm T}$ is analysed starting from the transformation matrix relating $\mathbf{L}_{\rm ind}$ and $\mathbf{L}_{\rm T}$. Because the pair $(hkl)/[uvw]$ is quasi-perpendicular (within $\omega_{\rm UL}$), $\mathbf{L}_{\rm T}$ is at least pseudomonoclinic. In terms of the primitive cell, the transformation is straightforward:

[7] For information on the possibility of zero-obliquity TLQS twins, see the discussion of the leucite case in Grimmer & Nespolo (2006).

$$\left\langle a \quad b \quad c \right|_{\mathbf{L}_T} = \left\langle a^P \quad b^P \quad c^P \right|_{\mathbf{L}_{ind}} \mathbf{U}_T^P; \quad \mathbf{U}_T^P = \begin{bmatrix} u_A^P & u_T^P & u_B^P \\ v_A^P & v_T^P & v_B^P \\ w_A^P & w_T^P & w_B^P \end{bmatrix}. \tag{6}$$

The same transformation is obtained from the conventional cell (the cell normally given in input by the user) by considering the coordinates $x_A y_A z_A$, $x_B y_B z_B$ and $x_T y_T z_T$ (which can be fractional) of the first node along the corresponding directions in the conventional mesh in (*hkl*) and along the direction quasi-perpendicular to the (*hkl*) plane. The transformation from $\mathbf{L}_{ind}$ to $\mathbf{L}_T$ is then obtained from

$$\left\langle a \quad b \quad c \right|_{\mathbf{L}_T} = \left\langle a \quad b \quad c \right|_{\mathbf{L}_{ind}} \mathbf{U}_T; \quad \mathbf{U}_T = \begin{bmatrix} x_A & x_T & x_B \\ y_A & y_T & y_B \\ z_A & z_T & z_B \end{bmatrix}. \tag{6'}$$

If m_{ind} and m_T are the multiplicities of the conventional cells of $\mathbf{L}_{ind}$ and of $\mathbf{L}_T$, respectively, and $|\mathbf{U}_T|$ is the determinant of the transformation matrix $\mathbf{U}_T$, the twin index is simply $n = |\mathbf{U}_T| \times m_{ind}/m_T$.

The computed obliquity is assumed to be an angular tolerance on the metric symmetry of $\mathbf{L}_T$, whereas the tolerance on the linear parameters is chosen by the user. The evaluation of the pseudosymmetry of $\mathbf{L}_T$ is described by the following examples.

1. If the obliquity of the sublattice is 1.5° and $\mathbf{L}_T$ is monoclinic with $\beta \leq 91.5°$, $\mathbf{L}_T$ is considered pseudo-orthorhombic, whereas it is considered monoclinic if $\beta > 91.5°$.

2. If $\mathbf{L}_T$ is orthorhombic with $|a - b| \leq t$, where t is the tolerance adopted by the user, then $\mathbf{L}_T$ is considered pseudo-tetragonal.

The type of centring of $\mathbf{L}_T$ is also evaluated as follows, starting from the *primitive* cell of $\mathbf{L}_{ind}$ (Grimmer & Nespolo, 2006):

1. if $u_A^P + u_T^P$, $v_A^P + v_T^P$, $w_A^P + w_T^P$ are all even, the lattice is *C*-centred;

2. if $u_B^P + u_T^P$, $v_B^P + v_T^P$, $w_B^P + w_T^P$ are all even, the lattice is *A*-centred;

3. if $u_A^P + u_B^P$, $v_A^P + v_B^P$, $w_A^P + w_B^P$ are all even, the lattice is *B*-centred;

4. if the three conditions above are all satisfied, the lattice is *F*-centred;

5. if $u_A^P + u_B^P + u_T^P$, $v_A^P + v_B^P + v_T^P$, $w_A^P + w_B^P + w_T^P$ are all even, the lattice is *I*-centred.

If the result is a non-standard setting (*e.g.* *a*-unique monoclinic lattice, *mA* or *mB* lattices *etc.*), the transformation to a standard setting is applied.

The same analysis can be applied to the other $\lambda - 1$ concurrent sublattices.

5. Examples

A few examples are analysed with some details in this section. These are all taken from mineral structures because of the large number of detailed descriptions of twins available in the literature for this category. Obviously, the analysis applies as well to any kind of triperiodic crystalline compound. Cell parameters have been taken from http://www.webmineral.com/.

Table 3
Analysis of the {012} twin in forsterite as a function of κ in $\Lambda(\kappa, 6°)$.

κ	$\lambda\kappa$	[*hkl*]	n	ω	n_E	$\tau[uvw]_\kappa/\tau[uvw]_{\kappa-1}$
1–9	0	–	–	–	–	–
10	1	[029]	10	4.4	10.0	–
11	2	[015]	11	2.5	5.5	1.002
		[029]	10	4.4		
12	3	[0,2,11]	12	0.9	4.0	1.15
		[015]	11	2.5		
		[029]	10	4.4		
13–24	4	[016]	13	0.5	3.2	1.031
		[0,2,11]	12	0.9		
		[015]	11	2.5		
		[029]	10	4.4		

5.1. The {052} twin in pyrite and galena

The analysis of this twin was presented in Nespolo & Ferraris (2005)[8] on the basis of the previous definition of n_E. The generalized definition we have introduced here implies a minor modification of the lattice interpretation of this twin.

Pyrite, FeS_2, has space group $Pa\bar{3}$, a = 5.417 Å. Besides the common spinel law {111}/⟨111⟩, twin index 3, Smolař (1913) reported several other twins, some of which are definitely non-Friedelian. Because the lattice of pyrite is cubic, twinning is always *i*-TLS and the cell of $\mathbf{L}_T$ is uniquely defined by {*hkl*}/⟨*hkl*⟩. The parameter n_{max} is also uniquely defined by X/f: there is no need to explore a region larger than $\Lambda(X/f, \omega_{UL})$ because the sublattice corresponding to zero obliquity is defined *a priori*.

The {052} twin has n = 29 and ω = 0: the cell of $\mathbf{L}_T$ is defined by the directions [052], [02$\bar{5}$] and [100]: $\mathbf{L}_T$ is obviously tetragonal, and twinning is by reticular merohedry. In the exploration for concurrent sublattices, the region to be analysed is $\Lambda(29, \omega)$, where ω is here taken equal to the Friedelian limit of 6° as usual. In $\Lambda(29, 6°)$, besides [052] two other directions quasi-perpendicular to (052) exist: [021] and [031], for which n = 6, ω = 4.8° and n = 17, ω = 3.4°, respectively. These three contributions give n_E = 4.8, which coincides with the estimation [equation (4)]: 29/(1 + 4 + 1). When interpreted as a hybrid twin, the {052} twin in pyrite comes out to have an effective twin index within the Friedelian limit.

Fig. 2 shows the (100) plane of $\mathbf{L}_{ind}$ and the corresponding projection of the cells $\mathbf{L}_T$, $\mathbf{L}_2$ and $\mathbf{L}_3$, based on the (052)/[052], (052)/[021] and (052)/[031] pairs, respectively: the cell of $\mathbf{L}_2$ is centred *S*, the others are primitive. [02$\bar{5}$] is the direction representing the trace of the (052) plane on (100). White, blue and red nodes belong to $\mathbf{L}_T$, $\mathbf{L}_2$ and $\mathbf{L}_3$, respectively; black nodes belong to $\mathbf{L}_{ind}$ only. The cell of $\mathbf{L}_T$ passing through the twin plane contains one node of $\mathbf{L}_T$, four nodes of $\mathbf{L}_2$ and one node of $\mathbf{L}_3$ that are thus restored or quasi-restored by the twin operation. The fraction of nodes of $\mathbf{L}_{ind}$ that are (quasi-)

[8] Table 1 in Nespolo & Ferraris (2005) contains an evident typo: the obliquity of the alternative sublattices of the pyrite twin is 4.8, as discussed in the text, and not 5.5.

Table 4
Interpretation of the high-index twins in β-quartz.

Exploration done in $\Lambda(4\text{–}40,6^\circ)$ for all twins but the Pierre-Levée, for which the region explored was $\Lambda(4\text{–}40,7^\circ)$ because of the high obliquity of $\mathbf{L}_3$. In bold type, Friedel's interpretation of the twin. See text for details.

Twin name	Breithaupt	Belowda Beacon	Wheal Coates	Cornwall	Pierre-Levée
Twin law	{1121}	{3032}	{2131}	{2021}	{2133}
$\Lambda(\kappa_{\min},\omega)$	$\Lambda(6,6^\circ)$	$\Lambda(4,6^\circ)$	$\Lambda(17,6^\circ)$	$\Lambda(7,6^\circ)$	$\Lambda(10,7^\circ)$
$\mathbf{L}_T$	**(11$\bar{2}$1)/[552]**	**(30$\bar{3}$2)/[211]**	**(21$\bar{3}$1)/[431]**	**(20$\bar{2}$1)/[632]**	**(21$\bar{3}$3)/[544]**
Twin index	6	4	6	7	13
Obliquity	0.7°	4.7°	2.9°	1.5°	2.1°
$\mathbf{L}_2$	(11$\bar{2}$1)/[221]	–	–	–	(21$\bar{3}$3)/[433]
Twin index	5	–	–	–	10
Obliquity	4.4°	–	–	–	2.3°
$\mathbf{L}_3$	–	–	–	–	(21$\bar{3}$3)/[322]
Twin index	–	–	–	–	7
Obliquity	–	–	–	–	6.5°
Effective twin index n_E	3.0	4.0	6.0	7.0	4.3

restored by twinning is thus 29/(1 + 4 + 1) = 4.8, namely the effective twin index.

The same twin has been reported in galena, which however has a *cF* lattice type ($Fm\bar{3}m$, a = 5.936 Å) instead of *cP* as in the case of pyrite. As a consequence, for $\mathbf{L}_2$ (052)/[021], we have n_1 = 12 instead of 6 and thus int(X_1/X_2) = int(29/12) = 2, $n_E = \langle n_E \rangle$ = 29/(1 + 2 + 1) = 7.2. The cell of $\mathbf{L}_T$ is centred *I*, the cells of $\mathbf{L}_2$ and $\mathbf{L}_3$ are centred *S*.

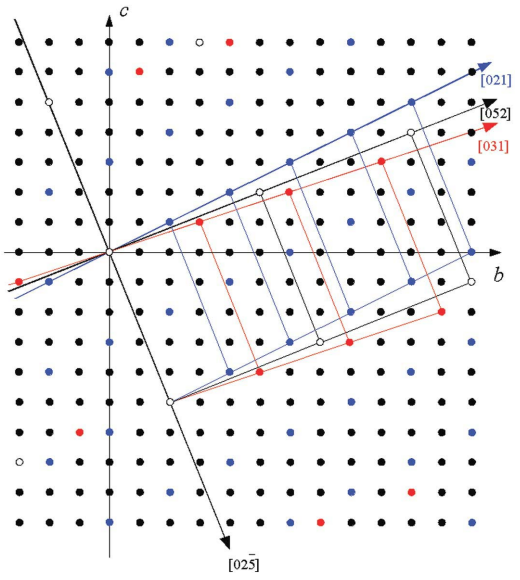

Figure 2
Interpretation of the {052} twin in pyrite as hybrid twin. The figure shows the (100) plane, which contains the direction [02$\bar{5}$] belonging to the twin plane and the three directions [021], [052] and [031] that are (quasi-) perpendicular to the twin plain (052). The white, blue and red nodes are (quasi-)restored, within $\omega = 6^\circ$, by the twin operation. The cell of $\mathbf{L}_T$ is univocally defined by the *i*-TLS character of this twin and is identified by the white nodes. This cell contains four blue nodes, belonging to the cell defined by the (052)/[021] pair, and one red node, belonging to the cell defined by the (052)/[031] pair. The overall degree of lattice quasi-restoration is 29/(1 + 4 + 1) = 4.8, and this is the effective twin index n_E for the {052} twin of pyrite.

5.2. The {012} twin in forsterite

Forsterite, Mg_2SiO_4, has space group *Pbnm*, a = 4.756, b = 10.195, c = 5.981 Å. In the literature, the {012} twin is reported, for which n = 13 (Palache *et al.*, 1952), whose geminographical analysis is given in Table 3. This twin has $\lambda = 0$ up to $\Lambda(9,6^\circ)$: it is clearly a non-Friedelian twin, which cannot be explained when adopting a limit on the twin index as high as 9. The number of concurrent sublattices increases regularly from $\Lambda(10,6^\circ)$ to $\Lambda(13,6^\circ)$, passing from $\lambda = 1$ to $\lambda = 4$, with a corresponding decrease in the effective twin index from 10.0 to 3.2: the direction defining the cell of $\mathbf{L}_T$ in $\Lambda(13,6^\circ)$ is [016]. No further change is observed up to $\Lambda(24,6^\circ)$. It is only at $\Lambda(25,6^\circ)$ that new contributions appear: the direction defining the cell of $\mathbf{L}_T$ would be [0,4,23] but the ratio $\tau_{[0,4,23]}/\tau_{[016]}$ is 1.95 ($\tau_{[0,4,23]}$ = 72.59, $\tau_{[016]}$ = 37.31 Å), showing that the new contributions would play a role only within a very large cell, with quasi-restored nodes far from the composition surface. This big gap clearly indicates that the best description of the (012) twin in forsterite is obtained by considering the $\lambda = 4$ sublattices in the $\Lambda(13,6^\circ)$ region.

The conventional mesh in (012) is defined by the two directions [02$\bar{1}$] and [100] that, together with [016], define a monoclinic primitive *c*-unique, pseudo-orthorhombic cell with parameters a = 21.249, b = 37.306, c = 4.756 Å, $\gamma = 90.49^\circ$. The transformation to the *b*-unique setting is thus obtained by

$$\left\langle a \quad b \quad c \right|_{\mathbf{L}_T} = \left\langle a \quad b \quad c \right|_{\mathbf{L}_{ind}} \mathbf{U}; \quad \mathbf{U} = \begin{bmatrix} 0 & -1 & 0 \\ 2 & 0 & 1 \\ -1 & 0 & 6 \end{bmatrix}.$$

$\mathbf{L}_T$ is pseudo-orthorhombic but differently oriented relatively to $\mathbf{L}_{ind}$, twinning is thus by reticular pseudo-polyholohedry[9].

5.3. High-index twins in β-quartz

Drugman (1927, 1928, 1930, 1939) performed a systematic study of twins in β-quartz and reported several examples of

[9] Reticular polyholohedry corresponds to the case in which the point symmetries of $\mathbf{L}_T$ and $\mathbf{L}_{ind}$ coincide but the two lattices have different orientations (see Nespolo & Ferraris, 2004*a*).

Table 5
Analysis of the {241} twin in diaphorite in different $\Lambda(\kappa,6^\circ)$ regions.

κ	$\lambda\kappa$	$[hkl]$	n	ω	n_E	$\tau[uvw]_\kappa/\tau[uvw]_{\kappa-1}$
1–6	0	–	–	–	–	–
7	1	[216]	7	5.6	7.0	–
8–14	2	[218]	8	2.7	4.0	1.13
		[216]	7	5.6		
15–30	6	[217]	15	1.4	1.9	1.69
		[7,3,26]	13	3.6		
		[7,3,22]	12	3.4		
		[5,3,22]	11	4.9		
		[5,3,18]	10	5.5		
		[218]	8	2.7		
		[216]	7	5.6		

Table 6
Analysis of the {032} twin in chalcocite in different $\Lambda(\kappa,6^\circ)$ regions.

κ	$\lambda\kappa$	$[hkl]$	n	ω	n_E	$\tau[uvw]_\kappa/\tau[uvw]_{\kappa-1}$
1–8	0	–	–	–	–	–
9	1	[326]	9	3.4	9.0	–
10–18	2	[326]	10	3.3	5.0	1.12
		[427]	9	3.4		
19–	4	[7,4,13]	19	2.0	3.8	1.64
		[214]	11	4.1		
		[326]	10	3.3		
		[427]	9	3.4		

high-index twins. As shown in Table 4, two of these twins are better interpreted as hybrid twinning.

The *Breithaupt* twin $\{11\bar{2}1\}$ is a Friedelian twin that is better described as a hybrid twin, with two concurrent sublattices: $\mathbf{L}_T$, defined by $(11\bar{2}1)/[552]$, and $\mathbf{L}_2$, defined by $(11\bar{2}1)/[221]$. The effective twin index is 3.0. Either $\mathbf{L}_T$ or $\mathbf{L}_2$ alone would suffice to describe this twin as Friedelian. The first sublattice is the one that would most naturally be chosen from inspection of the diffraction pattern. As anticipated in the §2.2, Friedel (1923) used both pairs in the same article but when both sublattices are considered together one obtains a better description of the lattice quasi-restoration.

The *Belowda Beacon* twin $\{30\bar{3}2\}$ is a Friedelian twin with twin index 4 and obliquity 4.7°, the quasi-perpendicular direction being [211]. No hybrid contribution exists up to $\Lambda(15,6^\circ)$, where the quasi-perpendicular direction would be [843] ($n = 15$, $\omega = 2.2^\circ$). The large gap from the $\Lambda(4,6^\circ)$ region clearly shows that this is not a hybrid twin: in fact, $\tau_{[843]}/\tau_{[221]} = 2.124$. The same type of argument applies to the Wheal Coates twin $\{21\bar{3}1\}$ and the Cornwall twin $\{20\bar{2}1\}$.

The *Pierre-Levée* twin $\{21\bar{3}3\}$ is not Friedelian. Drugman (1928) did not give the quasi-perpendicular direction but described this twin as having an index much larger than usual:[10] this suggests Drugman's choice of the pair $(21\bar{3}3)/[544]$, corresponding to $n = 13$ and $\omega = 2.1^\circ$. However, not far from [544], two alternative rational directions exist: [433] and [322], which correspond to indices 10 and 7, respectively. The last direction has a slightly non-Friedelian obliquity (6.5°) but its contribution to the hybrid twin is hardly deniable. If we take the pair $(21\bar{3}3)/[544]$ as the one defining the $\mathbf{L}_T$ sublattice, the overall degree of lattice restoration increases to $n_E = 4.3$, a Friedelian value. Further sublattices would appear only in correspondence of [977], with ratio $\tau_{[977]}/\tau_{[544]}$ of 1.6.

5.4. The {104} twin in pyrargyrite

Pyrargyrite, Ag_3Sb_3, has space group $R3c$, $a = 11.047$, $c = 8.719$ Å. Palache *et al.* (1952) describe a {104} twin which would correspond to a non-Friedelian twin with $n = 7$, $\omega = 0.5^\circ$ if only the lowest obliquity direction, [2,1,10], were considered. Not far from this direction another one exists, [217], which makes 4.6° with the normal to (104) and defines a sublattice with $n = 5$. Taken together, these two concurrent sublattices define a hybrid twin with effective twin index 3.5. No further sublattices exist in a region as wide as $\Lambda(30,6^\circ)$. The $\mathbf{L}_T$ sublattice is *mC* pseudo-orthorhombic, with parameters $a = 13.083$, $b = 11.047$, $c = 29.755$ Å, $\beta = 90.46^\circ$. Twinning is by reticular pseudomerohedry. The $\mathbf{L}_2$ sublattice is *mI* pseudo-orthorhombic, with parameters $a = 21.321$, $b = 11.047$, $c = 13.083$ Å, $\beta = 94.57^\circ$ and corresponds again to twinning by reticular pseudomerohedry.

5.5. Diaphorite twins

Diaphorite, $Pb_2Ag_3Sb_3S_8$, is a pseudo-orthorhombic sulfosalt with space group $C2_1/a$, $a = 15.84$, $b = 32.08$, $c = 5.9$ Å, $\beta = 90.165^\circ$. Two twins have been reported in diaphorite (Palache *et al.*, 1952): {120} and {241}. The first one is a normal Friedelian twin with $n = 4$ and $\omega = 0.7$, the quasi-perpendicular direction being [210]. The second twin is a hybrid twin that we analyse with some details.

Up to $\Lambda(6,6^\circ)$, no quasi-perpendicular direction to (241) exists, within 6° of obliquity, The first quasi-perpendicular lattice row occurs in $\Lambda(7,6^\circ)$: it is [216], for which $n = 7$ and $\omega = 5.6^\circ$. At this stage of description, the twin is simply non-Friedelian. Not far from this direction, another quasi-perpendicular lattice row exists, [218], for which $n = 8$ and $\omega = 2.7^\circ$. The period along these two directions is $\tau_{[218]} = 36.04$ and $\tau_{[216]} = 31.94$ Å, the ratio $\tau_{[218]}/\tau_{[216]}$ being 1.13.

No further sublattices are found in the region $\Lambda(9–14,6^\circ)$. However, in correspondence of $\Lambda(15,6^\circ)$, the lattice direction making the smallest obliquity becomes [217], which corresponds to ($n = 15$, $\omega = 1.4^\circ$). The corresponding period is $\tau_{[216]} = 61.08$ Å. If [217] is accepted as the direction defining $\mathbf{L}_1 = \mathbf{L}_T$, then not only the two directions previously found in $\Lambda(8,6^\circ)$ but also all the other directions with $n < 15$ and $\omega > 1.4^\circ$ have to be taken into account. These are listed in Table 5 . However, the increase from $\tau_{[218]}$ to $\tau_{[217]}$ is abrupt and clearly shows that the lattice node quasi-restored along this direction is much farther from the composition surface than the one on [218]. This is expressed by the ratio $\tau_{[217]}/\tau_{[218]} = 1.69$. A satisfactory description of the degree of quasi-restoration is given by the two sublattices in $\Lambda(8,6^\circ)$.

The conventional mesh in (241) is defined by the two directions $[10\bar{2}]$ and $[1\bar{1}2]$ that, together with [218], define a

[10] '*la macle de Pierre-Levée … aurait un indice beaucoup plus élevé que de coutume*' (Drugman, 1928, p. 190).

triclinic, pseudomonoclinic C b-unique cell with parameters a = 19.779, b = 65.207, c = 18.829 Å, α = 89.38, β = 98.62, γ = 87.50°. Twinning is by reticular pseudopolyholohedry. $\mathbf{L}_2$ is of the same type but with parameters a = 19.779, b = 57.266, c = 18.829 Å, α = 92.98, β = 98.62, γ = 94.23°.

5.6. Chalcocite twin

Chalcocite, Cu_2S, is a sulfide with space group $P2_1/c$, a = 11.881, b = 27.323, c = 13.491 Å, β = 116.35°. The {032} twin reported by Palache *et al.* (1952) has n = 9 and ω = 3.4°, the quasi-perpendicular direction being [326]. Not far from this direction, there is another one, [427], which corresponds to n = 10 and ω = 3.3°. Further increase in the number of concurrent sublattices λ is obtained only from $\Lambda(19,6°)$, with $\tau_{[uvw]k}/\tau_{[uvw]k-1} = \tau_{[7,4,13]}/\tau_{[326]}$ = 1.64 ($\tau_{[7,4,13]}$ = 101.16, $\tau_{[326]}$ = 61.56 Å). The {032} twin in chalcocite is thus interpreted as an n_E = 5.0 hybrid twin where two sublattices contribute significantly to the lattice quasi-restoration. The conventional mesh in (032) is defined by the two directions [100] and [2$\bar{2}$3] that, together with [427], define a pseudomonoclinic C-centred b-unique cell with parameters a = 65.842, b = 100.891, c = 11.881 Å, α = 93.19, β = 95.05, γ = 89.00°. Twinning is by reticular pseudopolyholohedry. $\mathbf{L}_2$ is of the same type but with parameters a = 11.881, b = 90.817, c = 65.842 Å, α = 86.58, β = 95.05, γ = 90.18°. See Table 6.

5.7. Klockmannite twin

Taylor & Underwood (1960) reported an i-TLS twin with n = 13 in klockmannite, CuSe ($P6_3/mmc$, a = 3.938, c = 17.25 Å). The twin plane is (13$\bar{4}$0) and the perpendicular direction is [570] (n = 13, ω = 0°). The geminographical analysis shows that in $\Lambda(13,6°)$ λ = 2: the alternative sublattice is based on (13$\bar{4}$0)/[230], which corresponds to n = 11 and ω = 3.0°. This second sublattice brings the effective twin index to a much more reasonable value, 6.5. $\mathbf{L}_T$ is oC, a = 14.199, b = 24.593, c = 17.250 Å; twinning is by reticular merohedry. $\mathbf{L}_2$ is mP pseudo-orthorhombic with parameters a = 14.199, b = 17.250, c = 10.419 Å, β = 93.00° and corresponds to twinning by reticular pseudomerohedry.

5.8. Misorientation of rhombohedral lattice with Σ = 5

Grimmer & Kunze (2004) applied the theory of coincident-site lattices (CSL) to the analysis of twinning by reticular pseudomerohedry. Their Table 9 gives the pairs $(hkl)/[uvw]$ for sublattices of rhombohedral $\mathbf{L}_{ind}$ corresponding to twin index 5 (the Σ factor in the CSL theory plays the role of the twin index in the reticular theory of twinning) as a function of c/a (hexagonal axes). Some of the (hypothetical) twins in Table 9 are of special interest because of their hybrid nature, despite the Friedelian index. Here we take as representative example the case of the {101} twin for c/a = 0.4330 that we analyse in full detail.

The normalized lattice parameters in hexagonal axes (a = 1, c = 0.4330 Å) become a = 0.5951 Å, α = 114.316° in rhombohedral axes, and the twin plane becomes (100). The perpendicular direction is [10,7,7] ([6,3,24] in hexagonal axes), which corresponds to n = 5 (Σ = 5). Not far from it, two other directions exist, [322] ([217] in hexagonal axes) and [433] ([2,1,10] in hexagonal axes), which make 3.2 and 4.8°, respectively, with the normal to the twin plane; the corresponding twin indices are 3 and 2. Equation (3) gives an estimation of n_E as

$$\langle n_E \rangle = \frac{10}{\text{int}(10/10)2 + \text{int}(10/3)1 + \text{int}(10/4)2} = 1.1.$$

The nodes belonging to the three cells are:

- for $\mathbf{L}_T$ (f_1 = 2, I-centred cell): 10,7,7 and 544;
- for $\mathbf{L}_2$ [f_2 = 1, primitive cell, int(X_1/X_2) = 3]: 322, 644 and 966;
- for $\mathbf{L}_3$ [f_1 = 2, I-centred cell, int(X_1/X_2) = 2]: 433 and 222, 866 and 444.

To these nine nodes, the neighbours are added, obtained by adding and subtracting the vectors defining the primitive mesh in (001), namely [010] and [001], as well as their vector sum, [011]. The resulting nodes are expressed in the axial setting of $\mathbf{L}_T = \mathbf{L}_1$ [equation (5)]:

$$\begin{bmatrix} 0 & 10 & 0 \\ 0 & 7 & 1 \\ 1 & 7 & 0 \end{bmatrix}^{-1} \left| u \quad v \quad w \right\rangle_{\mathbf{L}_{ind}} = \left| u \quad v \quad w \right\rangle_{\mathbf{L}_T}.$$

Of the whole set of stored nodes, only eight nodes are independent and internal to the cell of $\mathbf{L}_T$, namely 222, 333, 433, 544, 655, 877, 977 and 10,7,7. The node 433 occurs twice: at the corner of the first cell of $\mathbf{L}_2$ and as [0$\bar{1}\bar{1}$] equivalent of the 444 node, namely the I-centring node of the second cell of $\mathbf{L}_2$. The effective twin index is therefore 10/8 = 1.2, only slightly higher than the estimation calculated above.

In a case like this, the effective twin index is close to 1 and twinning is thus close to pseudomerohedry, rather than to reticular merohedry. Of the eight quasi-restored nodes, six correspond to a non-zero obliquity and represent a hybrid contribution to the twin. Such a contribution would not exist for a slightly different value of the ratio c/a: we can conclude that a crystal with such a specialized metric will most likely have a significantly higher tendency to twin than other compounds with a less specialized metric.

6. Discussion

The above analysis is purely reticular, done in terms of $\mathcal{D}(\mathbf{L}_T)$ and $\mathcal{H}^* = \cap_i \mathcal{D}(\mathbf{L}_{ind})_i$. Actually, either the twin point group $\mathcal{K}$ or the individual point group $\mathcal{H}$ (or both) may be merohedral, (when $\mathcal{H}$ is holohedral $\mathcal{H}^*$ is centrosymmetric). Let us see what changes with respect to the analysis developed above.

- *The twin point group $\mathcal{K}$ is merohedral.* $\mathcal{D}(\mathbf{L}_T)$ no longer coincides with $\mathcal{K}$ but is a supergroup of it. If r is the ratio of the order of $\mathcal{D}(\mathbf{L}_T)$ and the order of $\mathcal{K}$, and q is the index of $\mathcal{H}^*$ in $\mathcal{D}(\mathbf{L}_T)$, then only q/r of the cosets obtained when decomposing $\mathcal{D}(\mathbf{L}_T)$ correspond to possible twin laws. The reduction of the number of possible twin laws affects the choice of the (supposed) twin element but has no effect on the analysis developed above. Evidently, if the twin element is parallel to a

symmetry element of $\mathcal{H}$, the above analysis reveals the non-parallel elements that are equivalent under $\mathcal{H}^*$. For example, if $\mathcal{K} = 4/m$ and $\mathcal{H}^* = 2/m$, the algorithm finds the four cosets of $\mathcal{D}(\mathbf{L}_T) = 4/mmm$ with respect to $\mathcal{H}^*$: two of them are $\mathcal{H}^*$ itself and the coset containing the fourfold operation about the twofold axis of $\mathcal{H}^*$.

• *$\mathcal{H}$ is merohedral*. Each of the q cosets splits into p cosets, where p is the index of $\mathcal{H}$ in $\mathcal{D}(\mathcal{H})$. The consequence is that additional twinning by merohedry with respect to $\mathcal{H}^* = \cap_i \mathcal{H}_i$ is also possible, but this does not influence the occurrence of the non-merohedric component(s) of the twin.

6.1. Example of $\mathcal{D}(\mathbf{L}_T) \supset \mathcal{K}$

Let $\mathcal{H} = \mathcal{H}^* = m$, $\mathcal{K} = 3m$, $\mathcal{D}(\mathbf{L}_T) = \bar{3}m$.[11] The coset decomposition of $\mathcal{D}(\mathbf{L}_T)$ and of $\mathcal{K}$ in terms of $\mathcal{H}^*$ are:

$\bar{3}m = \{1, m_{[010]}\} \cup \{3^+_{[001]}, m_{[110]}\} \cup \{3^-_{[001]}, m_{[100]}\} \cup \{2_{[100]}, \bar{3}^-_{[001]}\} \cup \{2_{[010]}, \bar{1}\} \cup \{2_{[110]}, \bar{3}^+_{[001]}\}$;

$3m = \{1, m_{[010]}\} \cup \{3^+_{[001]}, m_{[110]}\} \cup \{3^-_{[001]}, m_{[100]}\}$.

Of the $q = 6$ cosets obtained when decomposing $\mathcal{D}(\mathbf{L}_T)$ in terms of $\mathcal{H}^*$, only $q/r = 6/2 = 3$ remain for $\mathcal{K}$. The twin lattice is not influenced by the fact that $\mathcal{K}$ is merohedral.

6.2. Example of merohedral $\mathcal{H}$

Let $\mathcal{D}(\mathbf{L}_T) = \mathcal{K} = mmm$. When passing from $\mathcal{H} = 2/m$ (holohedral) to $\mathcal{H} = 2$ (merohedral), the number of cosets changes from 2 to 4:

$mmm = \{1, 2_{[010]}, \bar{1}, m_{[010]}\} \cup \{2_{[100]}, 2_{[001]}, m_{[100]}, m_{[001]}\}$

$mmm = \{1, 2_{[010]}\} \cup \{2_{[100]}, 2_{[001]}\} \cup \{\bar{1}, m_{[010]}\} \cup \{m_{[100]}, m_{[001]}\}$.

The third coset represents twinning by merohedry; the fourth one is equivalent to the second one in terms of the lattice: one or the other can be realized in a binary twin, both in the case of a four-individual twin.

6.3. Solving and refining crystal structures affected by hybrid twinning

The occurrence of more than one concurrent sublattice contributing to the (quasi-)restoration of lattice nodes concerns the post-solution description of the lattice restoration but not the usual procedures of unravelling diffraction patterns, either from a theoretical viewpoint (*cf.* Ferraris *et al.*, 2004) or *via* algorithms implemented in crystallographic packages (Herbst-Irmer & Sheldrick, 1998). In fact, the key to interpreting the diffraction pattern of a twin is the identification of a twin law which explains a substantial (quasi-) restoration of nodes (diffraction spots). Possible additional contributions *via* sublattices other than $\mathbf{L}_T$ concern the quasi-restoration of further nodes, which however are expected to be sufficiently separated in view of the higher obliquity. In other words, the hybrid nature of a twin may appear once the structure has been solved: it is only a matter of *description* of the twin itself but does not interfere with the process of structure solution and refinement.

It must also be considered that, owing to the low fraction $1/n$ of (quasi-)overlapped nodes in a non-Friedelian (high-index) twin, where hybrid twins have a higher chance to appear, the crystal structure of such twins can reasonably be solved even without detecting twinning. However, even a low percent of not detected overlapped diffracted intensities will negatively affect the refinement of the structure.

[11] The twin point groups should actually be described by a polychromatic symbol, see Nespolo (2004). For simplicity here we use the corresponding achromatic symbol.

7. Conclusions

The present analysis of hybrid twins, first introduced by Nespolo & Ferraris (2005), shows that the classical twin index fails to describe the actual degree of lattice (quasi-)restoration when more than one (quasi-)restored concurrent sublattices exist within the Friedelian limit on the obliquity.

Particularly remarkable is the fact that some degree of 'hybridization' is often present also in Friedelian twins, *i.e.* in twins with twin index not higher than 6 and obliquity not higher than 6° – see the *Breithaupt* twin in β-quartz described above. In these cases, $n_E < n$ and the probability of occurrence of the twin is reasonably higher for the same reason for which the appearance of several non-Friedelian twins is explained on the basis of the concurrence of more than one sublattice.

The Fortran program *GEMINOGRAPHY* described in this article performs a systematic search for non-merohedric twin laws through the analysis of (quasi-)perpendicular (*hkl*)/[*uvw*] pairs and it allows the hybrid twin components to be found in all kinds of non-merohedric twins. The program can be downloaded without charge at the web address: http://www.lcm3b.uhp-nancy.fr/lcm3b/Pages_Perso/Nespolo/geminography.php, where detailed instructions on how to prepare the input file and how to read the output file are also available.

We wish to express our gratitude to the anonymous reviewers whose critical remarks significantly improved the readability of our manuscript. GF acknowledges the Italian Ministry of University and Scientific Research (MIUR) for financial support.

References

Arnold, H. (2002). *International Tables for Crystallography*, Vol. A, 5th ed., edited by Th. Hahn, Section 5. Dordrecht/Boston: Kluwer Academic Publishers.
Buerger, M. J. (1945). *Am. Mineral.* **30**, 469–482.
Catti, M. & Ferraris, G. (1976). *Acta Cryst.* A**32**, 163–165.
Donnay, J. D. H. (1940). *Am. Mineral.* **25**, 578–586.
Donnay, J. D. H. & Donnay, G. (1959). *International Tables for X-ray Crystallography*, Vol. III, Section 3.1.9. Birmingham: Kynoch Press.
Donnay, G. & Donnay, J. D. H. (1974). *Can. Mineral.* **12**, 422–425.
Drugman, J. (1927). *Mineral. Mag.* **21**, 366–382.
Drugman, J. (1928). *Bull. Soc. Fr. Minéral.* **51**, 187–192.
Drugman, J. (1930). *Bull. Soc. Fr. Minéral.* **53**, 95–104.
Drugman, J. (1939). *Bull. Soc. Fr. Minéral.* **62**, 99–132.

Ferraris, G., Makovicky, E. & Merlino, S. (2004). *Crystallography of Modular Materials*. IUCr/Oxford University Press.
Friedel, G. (1904). *Étude sur les Groupements Cristallins*. Extrait du *Bullettin de la Société de l'Industrie Minérale*, Quatrième série, Tomes III et IV. Saint-Étienne: Société de l'Imprimerie Théolier J. Thomas et C.
Friedel, G. (1923). *Bull. Soc. Fr. Minéral.* **46**, 79–95.
Friedel, G. (1926). *Leçons de Cristallographie*. Nancy/Paris: Berger-Levrault.
Friedel, G. (1933). *Bull. Soc. Fr. Minéral.* **56**, 262–274.
Grimmer, H. (2003). *Acta Cryst.* A**59**, 287–296.
Grimmer, H. & Kunze, K. (2004), *Acta Cryst.* A**60**, 220–232.
Grimmer, H. & Nespolo, M. (2006). *Z. Kristallogr.* **220**, 28–50.
Hahn, Th. & Klapper, H (2003). *International Tables for Crystallography*, Vol. D, edited by A. Authier, Section 3.3. Dordrecht: Kluwer Academic Publishers.
Herbst-Irmer, R. & Sheldrick, G. M. (1998). *Acta Cryst.* B**54**, 443–449.
Holser, W. T. (1958). *Z. Kristallogr.* **110**, 249–265.
Koch, E. (1999). *International Tables for Crystallography*, Vol. C, 2nd ed., edited by A. J. C. Wilson, Section 1.3. Dordrecht: Kluwer Academic Publishers.
Le Page, Y. (2002). *J. Appl. Cryst.* **35**, 175–181.
Mighell, A. D. & Rodgers, J. R. (1980). *Acta Cryst.* A**36**, 321–326.
Nespolo, M. (2004). *Z. Kristallogr.* **219**, 57–71.
Nespolo, M. & Ferraris, G. (2000). *Z. Kristallogr.* **215**, 77–81.
Nespolo, M. & Ferraris, G. (2003). *Z. Kristallogr.* **218**, 178–181.
Nespolo, M. & Ferraris, G. (2004*a*). *Acta Cryst.* A**60**, 89–95.
Nespolo, M. & Ferraris, G. (2004*b*). *Eur. J. Mineral.* **16**, 401–406.
Nespolo, M. & Ferraris, G. (2005). *Z. Kristallogr.* **220**, 317–323.
Nespolo, M., Ferraris, G., Ďurovič S. & Takéuchi, Y. (2004). *Z. Kristallogr.* **219**, 773–778.
Palache, C., Berman, H. & Frondel, C. (1952). *The System of Mineralogy of James Dana and Edward Salisbury Dana*, 7th ed., Vol. I, third printing. New York: Wiley; London: Chapman.
Santoro, A. (1974). *Acta Cryst.* A**30**, 224–231.
Smolař, G. (1913). *Z. Kristallogr.* **52**, 461–500.
Spek, A. L. (1990). *PLATON, a Multipurpose Crystallographic Tool.* Utrecht University, Utrecht, The Netherlands.
Takeda, H., Donnay, J. D. H. & Appleman, D. (1967). *Z. Kristallogr.* **125**, 414–422.
Taylor, C. A. & Underwood, F. A. (1960). *Acta Cryst.* **13**, 361–362.
Wondratschek, H. (2002). *International Tables for Crystallography*, Vol. A, 5th ed, edited by Th. Hahn, pp. 719–740. Dordrecht: Kluwer Academic Publishers.